ELSEVIER

European Polymer Journal 37 (2001) 659–670

EUROPEAN POLYMER JOURNAL

Curing of cyanate ester resin: a novel approach based on FTIR spectroscopy and comparison with other techniques

P. Bartolomeo *, J.F. Chailan, J.L. Vernet

Laboratoire de Chimie Appliquée, Université de Toulon et du Var, BP 56, 83162 La Valette du Var Cedex, France

Received 28 April 2000; received in revised form 5 June 2000; accepted 24 July 2000

Abstract

The aim of this study is to demonstrate a new sampling methodology to study resin curing by Fourier transform infrared (FTIR) spectroscopy. The principle of this novel approach consists in curing resin directly into the KBr pellet. In this method, only one pellet is needed during the treatment time. This approach is validated in the case of isothermal curing. We investigate the effects of the chemical nature of the resin, the amount of catalyst and epoxy added. All results are compared with the previous literature data and are in excellent agreement. Curing measurements are validated by thermal data obtained by differential scanning calorimetry. Then, in the last part, kinetic constant of cyanate ester resin curing is calculated by means of FTIR experimental data, and kinetic model available in the literature is verified. This kinetic approach has allowed us to compare our FTIR data with dynamic mechanical and dielectric measurements. © 2001 Elsevier Science Ltd. All rights reserved.

Keywords: Thermosetting; Cyanate ester resin; Curing kinetics; Fourier transform infrared; Kinetic model

1. Introduction

Fourier transform infrared (FTIR) spectroscopy is now widely used to characterise thermosetting resin curing [1]. Theoretically, the principle of kinetic building consists in following the evolution of a reactive vibration band of the resin versus cure treatments, time and temperature. This evolution is related to a reference vibration band, whose intensity does not vary during the curing process. This methodology is well known as the internal reference method, and is currently used. Practically, samples are prepared from bulk curing resin, and by making either one KBr pellet per measurement point or a sandwich of the uncured resin between two NaCl or KBr plates. The aim of this study is to propose a new methodology of sample preparation to study thermosetting resin curing. The principle consists in making one KBr pellet of the uncured resin and curing it directly into the pellet. In this paper, results obtained with such a preparation are compared with the literature data, and other experimental techniques such as differential scanning calorimetry (DSC). Kinetic parameters are calculated and coupled with kinetic model available for cyanate ester system.

Curing mechanism of cyanate ester resin is understood [2,3]. This mechanism is illustrated further in this paper. Schematically, OCN functions of cyanate monomers first trimerise to form a trimer named triazine. Then, in the second step, triazine polymerises using OCN free functions. The aim of this work is not to study in detail all chemical mechanisms involved in cyanate ester reaction, but to highlight kinetic characterisation of cyanate ester curing.

2. Experimental

This study is included in an industrial program. The aim is to test a new methodology to characterise resin cure cycle, with low manufacturing cost. The company we work for is specialised in radome aircraft

* Corresponding author. Fax: +33-04-94142598.

0014-3057/01/$ - see front matter © 2001 Elsevier Science Ltd. All rights reserved.
PII: S0014-3057(00)00165-8

manufacturing. In the case of radioelectric applications, a low dielectric constant matrix must be chosen. In this way, thermosetting cyanate ester resins (from CIBA: AroCy M: bis(4-cyanato-3,5-dimethylphenyl)methane) and AroCy B: 2,2′(4-cyanatophenyl)isopropylidene) are considered in this study. Resin referred to as AroCy M10 corresponds to an AroCy M monomer and resins AroCy M30 and AroCy B30 correspond to a previous curing of about 30%. The diglycidyl ether of bisphenol A (DGEBA) as well as acetyl acetonate of chromium III are from Aldrich (99% purity). FTIR measurements are performed with a Nicolet spectrometer, using 64 scans with a 2 cm^{-1} resolution step. Samples are prepared using a KBr matrix, with about 2% weight of resin. To obtain a homogeneous pellet, KBr and resin are mixed and placed under 200 bars for 15 min. The pellet is then placed in an oven, at a given temperature and time. To monitor cyanate ester resin curing, the vibration band νCN of the OCN function is chosen at 2270 cm^{-1} [3,4]. The reference band is attributed to the aromatic C–H band in the 2900–2850 cm^{-1} region. In the case of cyanate ester/epoxy mixture, DGEBA reaction is calculated using the desperation of epoxy bridge, whose vibration is observed at 915 cm^{-1}. In each case, conversion of resin, referred to as α throughout the entire study, is calculated using Eq. (1):

$$\alpha = \left[\frac{A_{\text{reactive-band}}}{A_{\text{reference-band}}}\right]_{T,t} \Bigg/ \left[\frac{A_{\text{reactive-band}}}{A_{\text{reference-band}}}\right]_{T,t=0}, \qquad (1)$$

where A_i is the area of vibration band, T, the temperature of isothermal cure and t, the time of curing.

Thermal characterisation is obtained using a DSC92 from SETARAM. 10 mg of resin are first cooled to −50°C and then characterised by heating at 10 K min^{-1} until 350°C. Samples are first cured in an oven and then characterised. Dynamic mechanical analysis (DMA) are realised with a solid visco analyser RSA II from Rheometrics. Resin T_α relaxation is measured using the dual cantilever tool. The sample is heated from 20°C to 350°C at 2 K min^{-1}, and 1 Hz. The T_α relaxation temperature is taken at $\tan\delta$ maximum peak. Dielectric measurements were performed with a DEA 2970 dielectrometer from TA instruments. A ceramic single surface sensor based on a coplanar interdigitated comb like configuration of electrodes was used.

3. Results and discussion

3.1. Primary observations and explorations

As an example, Fig. 1 represents spectrum evolution of cyanate ester resin during curing. A decrease in the area of OCN band at 2270 cm^{-1} as well as an increase in the triazine function (cyclotrimerisation of cyanate function) can be noted. We can also observe that the reference band remains nearly constant throughout the treatment time. This good result is obtained thanks to the utilisation of the same pellet throughout the curing process.

In Fig. 2 are shown the evolution of conversion versus time and temperature of isothermal curing for the three components tested. We can observe that conversion increases with time under given isothermal conditions and with the temperature of isothermal cure. Moreover, a maximal conversion lesser than 1 is observed at full conversion, which depends on isothermal conditions. This phenomenon as well as the value of this conversion will be discussed later.

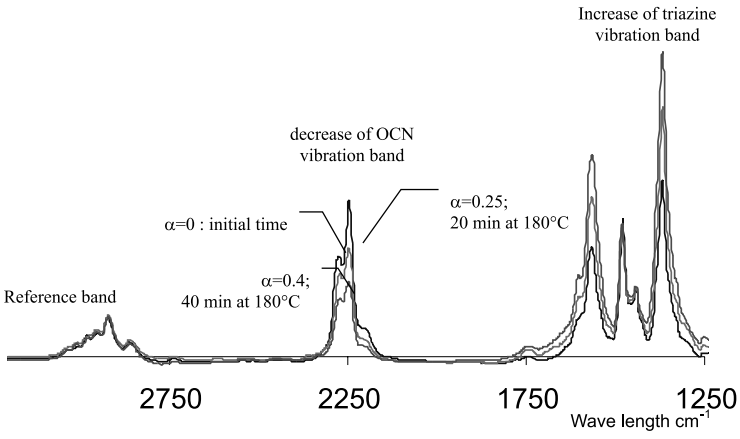

Fig. 1. Absorbance FTIR spectrum of an AroCy M30 resin at different curing conversions.

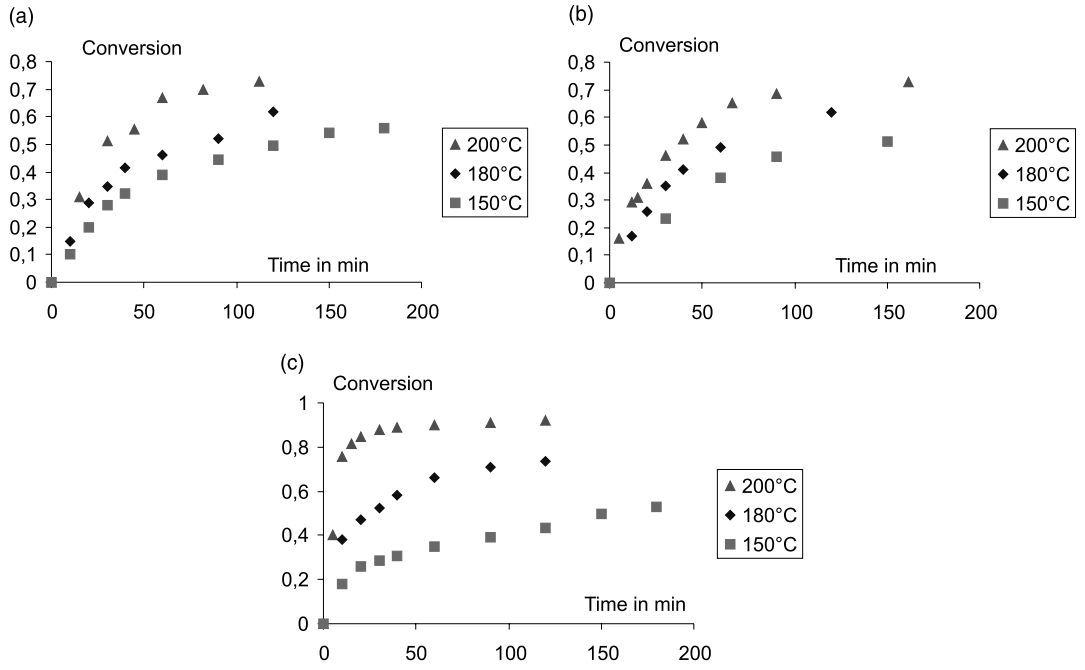

Fig. 2. Kinetic curve of conversion versus time and temperature of isothermal cure, in the case of (a) AroCy M10 resin, (b) AroCy M30 resin and (c) AroCy B30 resin.

3.2. Kinetic measurements

The presence of phenolic initiators and metal catalysts in the cyanate system strongly influence the kinetic evolution of the resin. In this way, some authors [5,6] have characterised such effects by considering a catalytic and an autocatalytic component. Then, they considered an expression of the kinetic law, reported in Eq. (2)

$$d\alpha/dt = (k_1\alpha + k_2)(1-\alpha)^n, \quad (2)$$

where $k_1\alpha$ is the autocatalytic component (significant when no metal catalyst is present [3]), k_2, the catalytic component. Only this must be considered for highly catalysed system, used in this study.

Moreover, it has been shown [7–9] that the catalytic constant is proportional to the amount of catalyst added in the media (Eq. (3)):

$$k_2 \rightarrow k_2[\text{catalyst}]. \quad (3)$$

Further, kinetic constants have been calculated. In each case, we have reported the evolution of the slope at initial time of the curve $\alpha(t)$ versus temperature by considering an Arrhenian relationship. Fig. 3 shows the evolution of ln(kinetic constant) versus $1/T$. A linear function is observed, and the calculations of activation energy and pre-exponential factor are given in Table 1. It is difficult to compare these data to those in the literature since we have got a commercial highly catalysed system. Nevertheless, Hamerton [10] has mentioned that in the case of similar experimental conditions, AroCy B

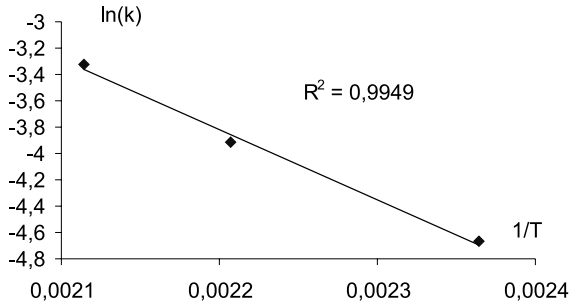

Fig. 3. Determination of Arrhenius catalytic constant parameters for AroCy M30 resin curing.

Table 1
Arrhenius kinetic parameter of catalytic constant

	AroCy M10	AroCy M30	AroCy B30
Activation energy ($J\,mol^{-1}$)	40 620	44 380	50 520
$\ln A$ (min^{-1})	6.9	7.92	10.26
Correlation coefficient (R^2)	0.97	0.99	0.99

Table 2
Kinetic comparison between AroCy B30 resin and AroCy M30 resin

Temperature (°C)	AroCy B30 k (min^{-1})	AroCy M30 k (min^{-1})	k_{B30}/k_{M30}
150	0.017	0.0094	1.8
180	0.04	0.02	2
200	0.08	0.036	2.2

Table 3
Effect of the amount of catalyst added on kinetic behaviour of two cyanate ester resin

	AroCy M30	AroCy B30
$k_{[Cat]} = 0.065\%$ (min^{-1})	0.02	0.023
$k_{[Cat]} = 0.13\%$ (min^{-1})	0.038	0.04
$k_{[Cat]} = 0.13\%/k_{[Cat]} = 0.065\%$	1.90	1.75

resins are cured with kinetics twice as that of AroCy M resins. Table 2 shows the comparison between the kinetic constants of AroCy M30 and AroCy B30 resins under the same curing conditions. We can observe that whatever the temperature of curing be ratio k_{B30}/k_{M30} is still nearly 2. This can be analysed in first approximation by the fact that our sampling mode does not affect kinetic conditions and properties of curing.

The systems we have got are catalysed with a weight ratio of 0.065% of chromium III. In order to verify Eq. (3) in our work, we have studied the effects of the amount of catalysts added to the catalytic constant. In this way, AroCy M30 and AroCy B30 resins are cured using 0.0065% weight ratio of Cr III (reference system) and using 0.013% of Cr III. Kinetic curve obtained at 180°C is shown in Fig. 4, and the experimental data are given in Table 3. Results show that the kinetic constant is approximately twice greater when the amount of catalyst was doubled. A good agreement is then obtained with the literature data [11].

3.3. Effect of epoxy monomer addition: kinetic and reaction mechanism

In the case of industrial use, cyanate ester resin are often mixed with epoxy resin [4]. In this section, we study the effect of an epoxy monomer addition to the system, and compare data obtained in bulk curing conditions.

It has been shown that epoxy monomer can induce a catalytic effect of the cyanate ester curing. This phenomenon is attributed to hydroxyl impurity carried by the epoxy monomer. Such an effect has been observed in our system. For instance, two concentrations of epoxy have been tested: 10% and 25% weight ratio. Kinetic curves at 180°C are shown in Fig. 5a for AroCy M10 resin, and Fig. 5b for AroCy M30 resin. We can observe that conversion increases with the amount of epoxy, which is characteristic of a catalytic behaviour. This observation has already been mentioned by Kim [12]. In the same way, kinetics of epoxy consumption increases with the amount of DGEBA added. To quantify the catalytic effect of epoxy component, we have plotted in Fig. 6 the evolution of the catalytic constant of cyanate ester curing versus the amount of epoxy added. $k_{0\%}$ is the catalytic constant of the neat resin, when no epoxy is added. A linear interpolation can be plotted, characteristic of a catalytic behaviour, as mentioned before.

On the one hand, we have just shown that the sampling mode does not affect the kinetic behaviour of cyanate ester–epoxy resin. On the other hand, we have observed that the mechanism on the reaction between cyanate and epoxy monomers can be characterised by means of our technique.

Reaction mechanism and cross-reaction between cyanate and epoxy resins have already been studied [4,10,13]. Here, the authors have proposed a reaction mechanism divided into four main steps and summarised in Fig. 7:

step 1: cyanate cyclotrimerisation – triazine band at 1370 and 1560 cm^{-1};
step 2: insertion of diglycidyl ether group in the cyanurate cycle – alkylcyanurate;

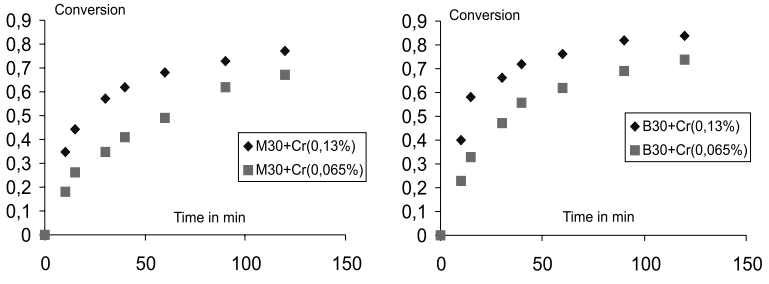

Fig. 4. Kinetic curve for AroCy M30 and AroCy B30 resins curing versus time and the amount of metal catalyst added. Curing temperature = 180°C.

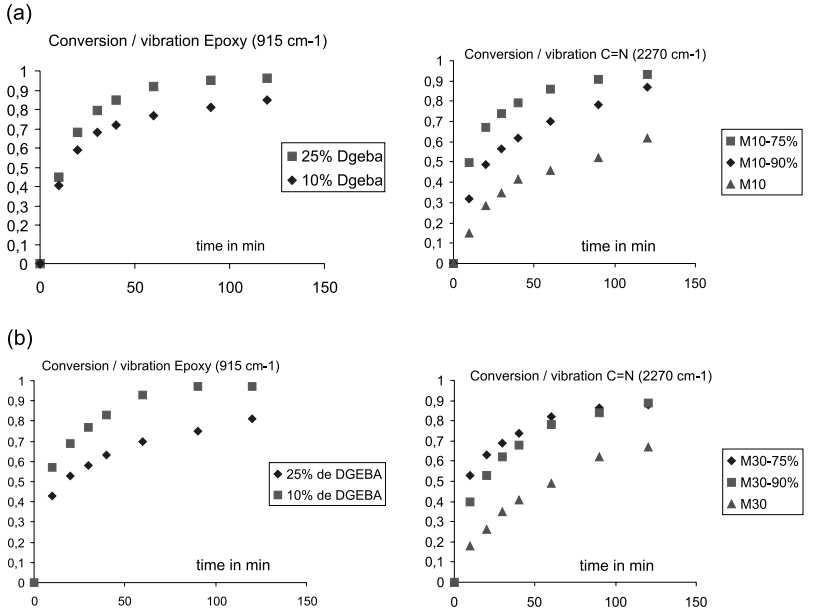

Fig. 5. Kinetic evolution curve of epoxy and OCN group versus time and amount of epoxy added. Isothermal curing at 180°C. (a) M10-X% is for a weight ratio of X% of AroCy M10 resin and $(100 - X)$% of DGEBA monomer, and (b) M30-X% is for a weight ratio of X% of AroCy M30 resin and $(100 - X)$% of DGEBA monomer.

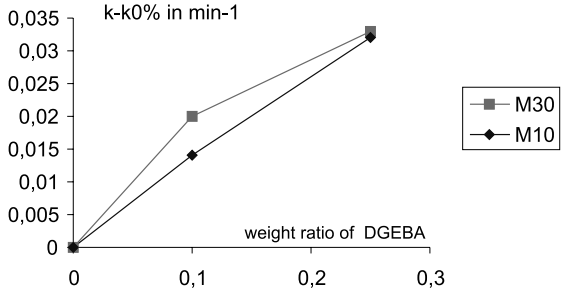

Fig. 6. Influence of the amount of epoxy added on the catalytic constant. k is the catalytic constant measured, and $k_{0\%}$ is the catalytic constant of reaction without DGEBA.

step 3: isomerisation of alkylcyanurate into alkylisocyanurate – 1684 cm^{-1} and
step 4: reaction of epoxy bridge on alkylisocyanurate – oxalolidinone at 1770 cm^{-1}.

It is possible to monitor the evolution of each step of the reaction by FTIR. As an example, Fig. 8 represents the FTIR spectrum (in the range of 1900–1625 cm^{-1}) of a mixture AroCy B30 75% and epoxy 25% cured under isothermal conditions at 180°C. We can experimentally observe the evolution of isocyanurate and oxalolidinone band versus time of treatment. The former increases with time, whereas the latter first increases and then decreases. Fig. 9 shows the evolution of all reactive bands versus time. For comparison, areas of all reactive bands are normalised to their maximum value during the cure. We can observe that the mechanism is first led by the reaction of cyanurate cycle to give the isocyanurate after rearrangement. As soon as some isocyanurate has been formed, a second reaction takes place to form the oxalolidinone group. Then, isocyanurate decreases until there is a lack of epoxy monomers.

In this section, we have shown that the reactions between cyanate and epoxy (due to oxalolidinone formation) still take place in the KBr pellet. Moreover, evolution mentioned are in good agreement with the literature data [14].

Until now, we have demonstrated that all observations made in the case of bulk curing condition were observed by curing the resin directly into the KBr pellet. It will be seen later that the data we obtained by FTIR spectroscopy can be correlated to bulk data, and especially, thermal data.

3.4. Comparison with thermal analysis

The aim of this section is to show that FTIR data can be easily linked to thermal data obtained by DSC. This study is organised by AroCy M30 characterisation, which acts as the reference resin of the study.

Conversion is deduced from DSC data by measuring the area of exothermal peak of partially cured samples

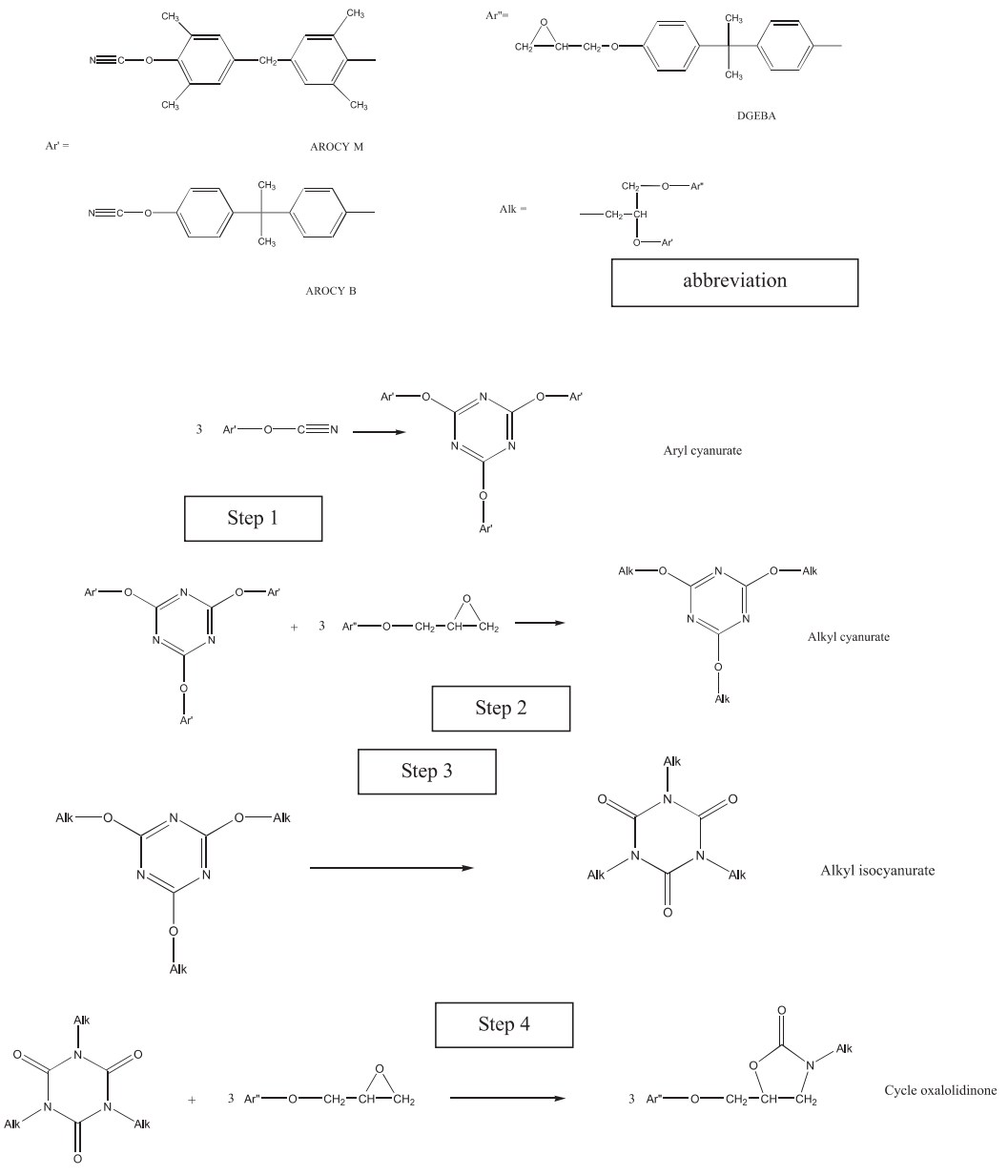

Fig. 7. Reaction mechanism between cyanate ester resin and epoxy monomer.

(at T, during t), and reporting it to the reference exothermic peak of uncured sample (Eq. (4))

$$\alpha = 1 - [\text{area}(T,t)/\text{area}(t=0)], \tag{4}$$

where area (T,t) represents the area of the residual exothermic peak after the sample has been cured during t under an isothermal T temperature. Area $(t=0)$ is representative of the uncured sample.

Some examples of experimental thermogram are shown in Fig. 10a (AroCy M10 monomer) and b (partially cured resin). In the first case, we can observe some catalyst and initiator manifestations (small undulations) at the beginning of the exothermic peak, as mentioned by Barton [15]. In the second case, it is possible to measure the T_g of the partially cured resin, observed at the baseline jump.

On one side, kinetic results extrapolated from the thermal methodology are reported in Fig. 11 in comparison with FTIR data. We can observe an excellent correlation between those two kinds of approach whatever be the temperature of curing. Similar kinetic

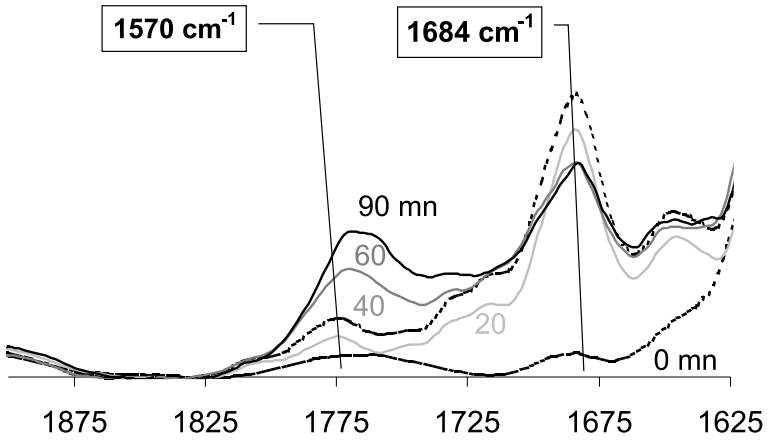

Fig. 8. FTIR spectrum of a AroCy B30 75% weight ratio and DGEBA 75% weight ratio in the range of 1900–1625 cm^{-1}. Evolution of vibration band of isocyanurate and oxalolidinone versus time for isothermal curing at 180°C.

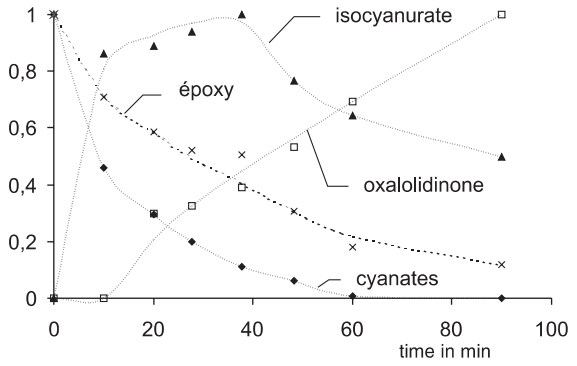

Fig. 9. Evolution of reactive entities in the case of AroCy B30 75% weight ratio and DGEBA 25% weight ratio versus time. Isothermal curing at 180°C.

curves and maximal conversions are obtained. On the other hand, taking account of the DSC T_g measurement data, we have been able to plot the evolution of T_g versus α. Since T_g measurements are no longer possible for high conversion state, in this case, T_g has been obtained by DMA measurements. Fig. 12 shows the evolution of T_g for the AroCy M30 resin versus conversion. Data are obtained by DSC for low conversion, and by DMA for high conversion. Moreover, the evolution of $T_g(\alpha)$ is well fitted by the Pascault–William law [16], mentioned:

$$T_g(\alpha) = T_{g_0} + \frac{(T_{g_\infty} - T_{g_0})\lambda\alpha}{1-(1-\lambda)\alpha}, \quad (5)$$

where T_{g_0} is the glass transition temperature of the uncured resin, $\alpha = 0$; T_{g_∞}, the glass transition temperature of the fully cured resin, $\alpha = 1$ and λ, a parameter that depends on the ratio of heat capacity jump at $\alpha = 1$ and $\alpha = 0$.

The experimental data fit leads to $T_{g_0} = 25$°C, $T_{g_\infty} = 293$°C and $\lambda = 0.29$, with an excellent correlation with reference data [3].

Thanks to those previous results, it is then possible to cross-link T_g measurements with maximal conversion and temperature of isothermal cure. In the case of the AroCy M30 resin, Table 4 represents for different curing temperatures the value of α_{max} measured by FTIR (which is the same as the value measured by DSC) as well as the corresponding measured glass transition temperature. We can observe a constant shift of about −50°C between the glass transition temperature and the

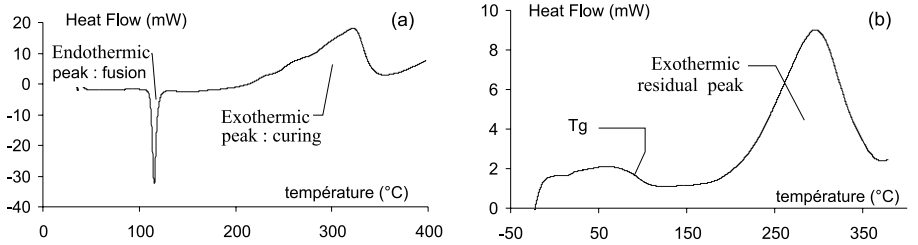

Fig. 10. Thermogram of (a) an AroCy M10 resin and (b) a partially cured sample.

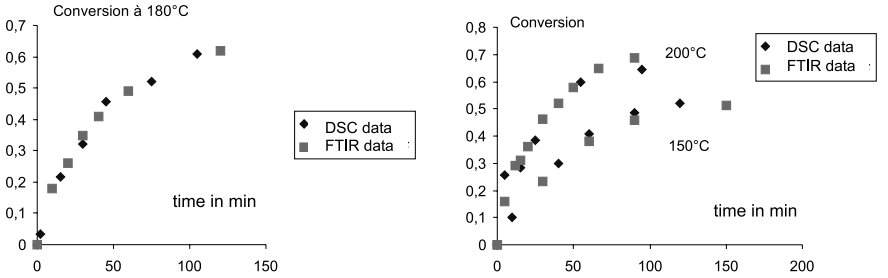

Fig. 11. Comparison between FTIR data and DSC data in the case of an AroCY M30 resin cured under isothermal conditions.

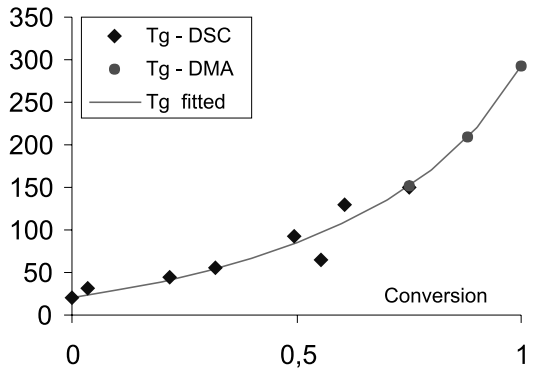

Fig. 12. Evolution curve of glass transition temperature versus conversion for an AroCy M30 cyanate ester resin. DSC and DMA data are represented and fitted by a Pascault–Williams relation.

Table 4
AroCy M30 resin: comparison of T_g and the maximal conversion at the end of cure

$T_{isotherm}$	150	180	200
α_{max}	0.53	0.68	0.75
$T_g(\alpha_{max})$	92	128	150
$T - T_g(\alpha_{max})$	58	52	50
α for $T_{iso} = T_g + 50$	0.58	0.69	0.75

Table 5
AroCy M30 resin: calculated parameter of Simon kinetic model

Temperature (°C)	180	200
A (min^{-1})	3.78×10^8	3.78×10^8
E_d ($kJ\,mol^{-1}$)	80 220	80 220
b	0.13	0.19

corresponding T_g:$T_{isothermal} = T_g + 50$°C. In the same way, the last row of Table 5 represents the calculated value of α_{max} when the previous relation is considered with Eq. (5). The calculated value is very close to the measured α_{max} obtained by FTIR. This observation has already been mentioned by Deng [17] in the case of catalysed cyanate ester system.

This observation demonstrates that the methodology developed in this study can be used as an absolute measurement of resin conversion, not only in the case of a relative investigation of resin curing. In other words, curing resin directly into the KBr pellet gives rise to the same results as curing resin in bulk conditions. This could be easily explained considering that resin into the pellet is organised as ''microbulk'', whose size is

- large enough to allow bulk conditions,
- small enough to allow a uniform repartition of the resin in the pellet.

This makes us think that this methodology is a good way to study resin curing, with a low cost of resin and low processing cost.

4. Kinetic model by means of Fourier transform infrared data

At the end of this study, we will interpret FTIR data to build the kinetic model for cyanate ester resin curing. We must keep in mind that thermosetting kinetic of cure is governed by two main phenomena. During the first stage of the reaction, kinetics of action of one reactive component to another one is limiting since reactive products are in excess in the bulk medium. Reaction is qualified under kinetic limitation. The second stage begins when characteristic time of action of one product becomes shorter than the time needed for a reactive component to reach the other one. The reaction is then said to be under diffusional limitation [17–20] due to the lack of product mobility, and kinetics of reaction decreasing versus conversion. In this case, a simple Arrhenius kinetic model (as mentioned in Eq. (2)) is available for low conversion but is no longer accurate for a high degree of conversion. In the last case, Eq. (2) must be rearranged to

$$d\alpha/dt = k_2(1-\alpha)^n g(\mu), \tag{6}$$

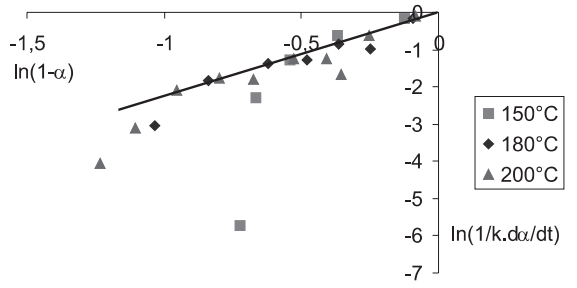

Fig. 13. Determination of the kinetic order of the curing reaction.

where $g(\mu)$ is the function of the mobility of products, $g(\mu) = 1$ for low conversion and $g(\mu)$ decrease until 0 for high conversion. To express $g(\mu)$, the authors use either $T_g(\alpha)$ evolution or free volume theory or diffusion coefficient calculation.

4.1. Reaction order determination

First, we have to calculate the order of the cyanate ester cure reaction. For this purpose, it is common to consider an Arrhenian evolution $d\alpha/dt = k(1-\alpha)^n$, which is available for the first step of the reaction. Then, the slope of the plot $\ln(1/k(d\alpha/dt))$ versus $\ln(1-\alpha)$ is equal to the order of the reaction n. Values of kinetic constant k are the slope of curves α versus time at initial time, as calculated in Table 2. Fig. 13 represents such a plot. We can observe a good linear interpolation for low conversion and a divergence between the experimental data and linear interpolation for high degree of cure. This is explained by the fact that the Arrhenian evolution is no longer available at the end of cure, because of the diffusional limitation of the reaction. Nevertheless, a reaction order of about 2 is measured, which fully agrees with the literature data [3].

4.2. Glass transition temperature limitation

In order to take care of limitation phenomenon, Stutz [21,22] has proposed a limitation based on T_g evolution versus conversion. Their model is given in the following equation:

$$\frac{d\alpha}{dt} = k_2(1-\alpha)^2 \exp\left[-\frac{E_s}{R}\left(\frac{1}{T - T_g(\alpha) + K} - \frac{1}{T - T_g(\alpha = 0) + K}\right)\right]. \quad (7)$$

This takes account of an activation energy, E_s, which represents the ability of a free segment to react with another one. E_s has been calculated to be about 1000 J in the case of an AroCy M resin. The value of the constant K has been optimised at $K = 0$. The fact that K is not equal to -50 (as expected from the data in Table 4) is a consequence of limitation phenomenon that occurs long time before the limit temperature. Fitted and experimental results are reported in Fig. 14. An excellent agreement is obtained between the experimental FTIR data and calculations.

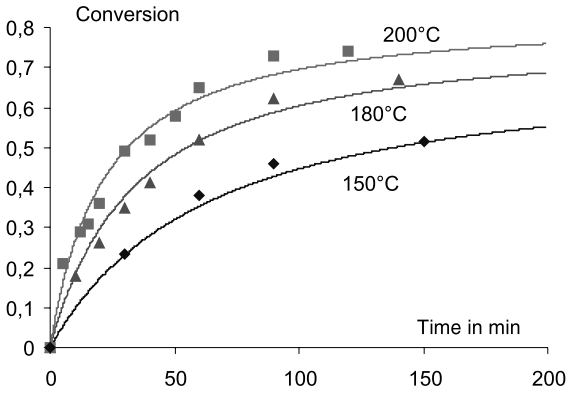

Fig. 14. AroCy M30 resin: kinetic curve fitted by a Stutz model (curing limitation by glass transition temperature evolution).

4.3. Diffusional limitation

Simon et al. [23] have proposed an approach based on free volume theory, considering that the limitation effect occurs long time before glass transition temperature limitation. They postulated that the inverse of kinetic constant is analysed as the sum of two main characteristic times: one of catalytic $1/k_c$ and another of diffusional nature $1/k_d$. With such considerations, the kinetic constant is given by

$$1/k = 1/k_c + 1/k_d. \quad (8)$$

The inverse of characteristic time of diffusion is a function of temperature and free volume as follows:

$$k_d = A \exp\left(-\frac{E_d}{RT_c}\right) \exp\left(-\frac{b}{f}\right), \quad (9)$$

where A and b are two empirical parameters, E_d, an activation energy of the diffusional process, T_c, the isothermal temperature of cure, and f, the free volume calculated as $f = 0.00048(T_c - T_g) + 0.025$.

The parameter determination is obtained by plotting $\ln(k_d)$ versus $1/f$. The slope of the linear interpolation gives b parameter, whereas the intercept is $\ln(A \exp(-E_d/RT_c))$. Then, using the three temperatures of the study, it is possible to calculate the activation energy, E_d and pre-exponential factor, A. Results are reported in Table 5. A good agreement is observed between the literature data for the b factor (0.2), whereas the couple (A, E_d) is lower. This can be explained by the

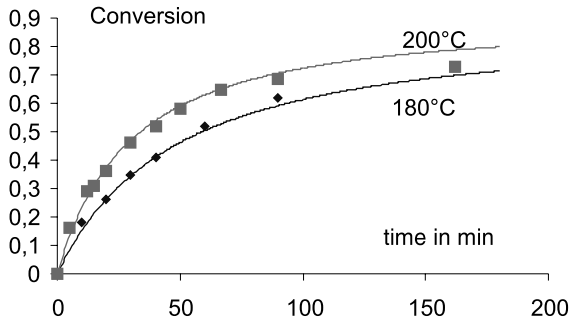

Fig. 15. AroCy M30 resin: kinetic curve fitted by a Simon model (curing limitation by diffusion).

fact that diffusion phenomena are stronger in case of those previous results, since the system studied is a RTX366. Those molecules have got three aromatic cycles in their rigid core, and they are sterically hindered.

An excellent agreement between experimental and fitted data can be seen in Fig. 15. Data obtained at 150°C are not represented since low limitation effects occur at this temperature. To conclude, we emphase on a cross-link correlation between FTIR data and dielectric data. As a matter of fact, Deng et al. [17,24] have taken care of diffusional limitations by measuring diffusion coefficient by means of dielectric data.

Their approach consisted of two main steps: A first step before 40% of conversion, where then reaction is driven by an Arrhenius law $(\mathrm{d}\alpha/\mathrm{d}t = k(1-\alpha)^2)$; no limitation occurs and a second step for conversion higher than 40% where diffusion phenomena are important. In the latter case, the kinetic constant is explained by

$$\frac{1}{k} \leftarrow \frac{1}{k} + \frac{D_{\alpha=0.25}}{k'_{\mathrm{d}0} D}, \tag{10}$$

where $k'_{\mathrm{d}0}$ is a constant, that is driven by an Arrhenius relation, D, the diffusion coefficient, and $D_{\alpha=0.25}$, the diffusion coefficient for $\alpha = 0.25$. The authors report that $D/D_{\alpha=0.25}$ ratio is equal to $\sigma/\sigma_{\alpha=0.25}$ ratio, where σ is ionic conductivity of the dielectric resin.

The principle of the dielectric technique consists in placing the sample under an alternative voltage, and measuring the resulting current and the phase angle shift induced. The measured current is separated into a capacitive and a conductive component. An equivalent capacitance and conductance are then calculated, and used to determine the dielectric permittivity, ε' and dielectric loss factor, ε''. ε' is proportional to capacitance and measures the alignment of dipoles. ε'' is proportional to conductance and represents the energy required to align dipoles and to move ions. The first term is representative of dipolar phenomena (α relaxation pro-

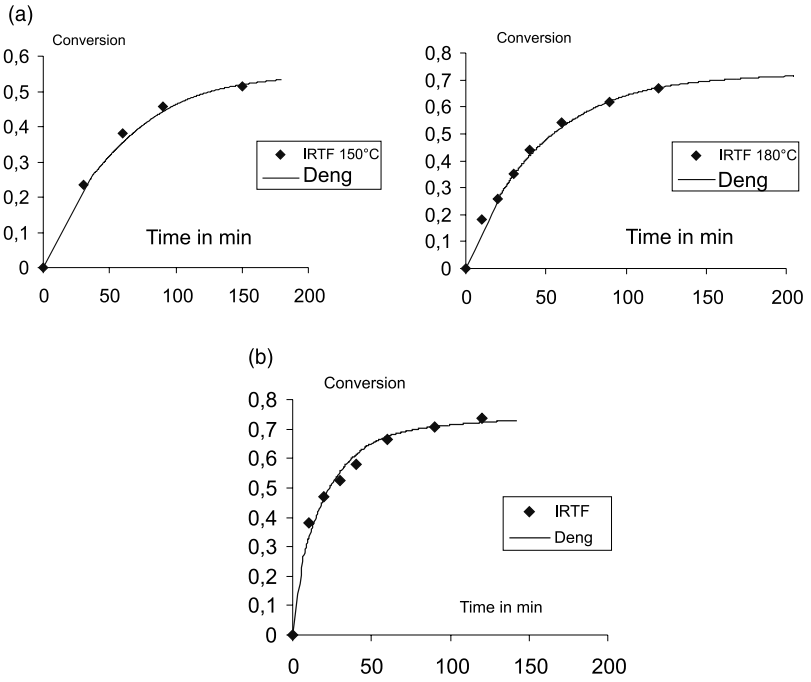

Fig. 16. (a) AroCy M30 resin: kinetic curve fitted by a Deng model (curing limitation by diffusion) – correlation between dielectric data and FTIR data at 150°C and 180°C. (b) AroCy B30 resin: kinetic curve fitted by a Deng model (curing limitation by diffusion) – correlation with dielectric data and FTIR data at 180°C.

Table 6
AroCy M30 resin: calculated Arrhenius parameter for the k'_{d0} constant for the Deng model comparison with AroCy B30 literature data

Resin	AroCy M30	AroCy B30 [17]
E_a (kJ mol^{-1})	227	203
A (min^{-1})	7.7×10^{27}	2.9×10^{26}

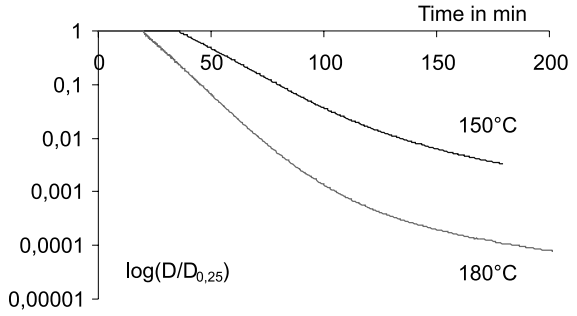

Fig. 17. AroCy M30 resin: logarithmic evolution of $D/D_{0.25}$ ratio versus time and temperature for isothermal curing.

cess), whereas the second term is proportional to σ. The ionic conductivity component used in this study is the direct current component, σ_{DC}. This is deduced from ε'' measurements using the Day method [25,26].

In Eq. (10), the catalytic constant k is the same as that calculated previously, and constant k'_{d0} is optimised to fit data with experimental points. In Fig. 16a and b experimental results corresponding to AroCy M30 and AroCy B30 curing are reported. Table 6 resumes the Arrhenian parameters of k'_{d0} constant, in comparison to the literature data. A good agreement is observed between the experimental and fitted data.

Further, we have plotted in Fig. 17, the evolution of the ratio $D/D_{\alpha=0.25}$ at two different temperature. We can observe that a strong and rapid decrease of the ratio occurs at 180°C. After 180 min of cure, the diffusion coefficient decreases to about four decades. In the same way, we have plotted the evolution of the ratio at 180°C versus time of AroCy M30 and AroCy B30 resins in Fig. 18. The same curve is observed, which means that if on the one hand, kinetic of cure is different for the two resins, on the other hand, the same diffusional process occur in the two media.

5. Conclusion

In this study, we have demonstrated the application of a new sampling method to monitor resin curing by FTIR. We have first focussed on the validation of this technique by showing that it was reliable in the case of

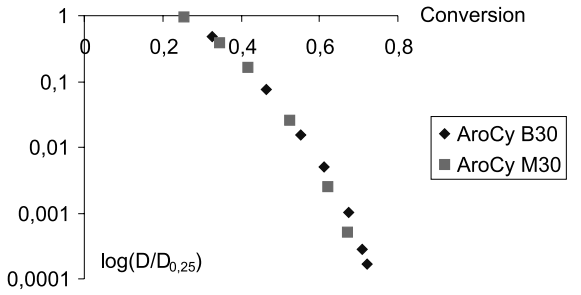

Fig. 18. Comparison of $D/D_{0.25}$ ratio versus curing conversion between an AroCy M30 and an AroCy B30 resin. Isothermal curing temperature, 180°C.

relative and absolute measurements. Then, those FTIR data have been used and tested according to kinetic model available in the literature on cyanate ester resin curing. The model and calculated parameters are in good agreement with FTIR and reference data. In conclusion, we must mention that this methodology has been correlated to other different techniques such as DSC and dielectric experiments. It could be very interesting to extend this study, based on cyanate ester resin to some other systems, such as thermosetting ones and thermoplastic solid state curing.

Acknowledgements

The authors would like to acknowledge the Ateliers Industriels de l'Aeronautique de Cuers Pierrefeu (AIA/CP) and Direction Generale de l'Armement (DGA) for financial support as well as Region Provence Alpes Côte d'Azur.

References

[1] Enns JB, Gillham JK. J Appl Polym Sci 1983;28:2567.
[2] Fyfe CA, Niu J, Rettig SJ, Burlinson NE, Reidsema CM, Wang DW, Poliks M. Macromolecules 1992;25:6289.
[3] Georjon O, Galy J, Pascault JP. J Appl Polym Sci 1993; 49:1441.
[4] Amon S. PhD dissertation, Lyon, 1995.
[5] Kenny JM, Opalicki M. Makromol Chem Macromol Symp 1993;68:41.
[6] Kenny JM, Berglund LA. SAMPE J 1991;27(2).
[7] Owusu AO, Martin GC. Polym Mater Sci Engng 1991; 65:304.
[8] Owusu AO, Martin GC, Gorto JT. Polym Mater Sci Engng 1991;31:1604.
[9] Owusu AO, Martin GC, Gorto JT. Polym Mater Sci Engng 1992;32:535.

[10] Hamerton I. Chemistry and technology of cyanate ester resins. NY: Blackie A & P, 1994.
[11] Owusu AO, Martin GC, Gotro JT. Polym Engng Sci 1992;32:385.
[12] Kim BS. J Appl Polym Sci 1997;65:85.
[13] Grenier-Loustalot MF, Lartigau C, Grenier P. Eur Polym J 1995;31(11):1139.
[14] Grenier-Loustalot MF, Lartigau C, Grenier P. Contrat DRET 91-1223A, 1993.
[15] Barton JM, Hamerton I, Jones JR. Polym Int 1992;29:145.
[16] Pascault PJ, Williams RJJ. J Polym Sci Polym Phys 1990; 28:85.
[17] Deng Y, Martin GC. Polymer 1996;37(16):3593.
[18] Owusu AO. PhD dissertation, Syracuse University, Syracuse, NY, 1992.
[19] Gallicher G, Galy J, Grenier MF, Mechin F, Bloch B, Dublineau P, Pascault JP, Stohr JF. Matériaux and Techniques 1996;7–8:31.
[20] Maffezzoli A, Trivisano A, Opalicki M, Mijovic J, Kenny JM. J Mater Sci 1994;29:800.
[21] Stutz H, Mertes J, Neubecker K. J Polym Sci: Part A: Polym Chem 1993;31:1879.
[22] Stutz H, Mertes J. J Polym Sci: Part A: Polym Chem 1993;31:2031.
[23] Simon JL, Gillham JK. J Appl Polym Sci 1993;47:461.
[24] Deng Y, Martin GC. J Appl Polym Sci 1997;64:115.
[25] Day DR, Lewis TJ, Lee HL, Senturia SD. J Adhesion 1985;18:73.
[26] Ciriscioli PR, Springer GS. 34th International SAMPE Symposium, 1989. p. 312.